

**Asteroid age distributions determined by space weathering
and collisional evolution models**

Mark Willman, Robert Jedicke

Institute for Astronomy, University of Hawai'i at Manoa
2680 Woodlawn Drive, Honolulu, HI 96822
willman@ifa.hawaii.edu, 808-956-6989 tel, 808-956-9580 fax
jedicke@ifa.hawaii.edu, 808-956-9841 tel, 808-956-9580 fax

23 pages

5 figures

1 table

ABSTRACT

We provide evidence of consistency between the dynamical evolution of main belt asteroids and their color evolution due to space weathering. The dynamical age of an asteroid's surface (Bottke *et al.* 2005; Nesvorný *et al.* 2005) is the time since its last catastrophic disruption event which is a function of the object's diameter. The age of an S-complex asteroid's surface may also be determined from its color using a space weathering model (*e.g.* Willman *et al.* 2010; Jedicke *et al.* 2004; Willman *et al.* 2008; Marchi *et al.* 2006). We used a sample of 95 S-complex asteroids from SMASS and obtained their absolute magnitudes and u, g, r, i, z filter magnitudes from SDSS. The absolute magnitudes yield a size-derived age distribution. The u, g, r, i, z filter magnitudes lead to the principal component color which yields a color-derived age distribution by inverting our color-age relationship, an enhanced version of the 'dual τ ' space weathering model of Willman *et al.* (2010).

We fit the size-age distribution to the enhanced dual τ model and found characteristic weathering and gardening times of $\tau_w = 2050 \pm 80$ Myr and $\tau_g = 4400_{-500}^{+700}$ Myr respectively. The fit also suggests an initial principal component color of -0.05 ± 0.01 for fresh asteroid surface with a maximum possible change of the probable color due to weathering of $\Delta PC = 1.34 \pm 0.04$. Our predicted color of fresh asteroid surface matches the color of fresh ordinary chondritic surface of $PC_1 = 0.17 \pm 0.39$.

Keywords: Asteroids, dynamics, surfaces

1. Introduction

During the twentieth century the number of known main belt (MB) asteroids jumped from less than 500 to nearly 20,000. The mushrooming inventory led to the discovery of asteroid families (Hirayama 1918) and the discovery of the colors of the main spectral types (Chapman *et al.* 1975). This was followed late in the century by the creation of an extensive database of colors by the Sloan Digital Sky Survey (SDSS (Abazajian *et al.* 2009)), making possible high statistics color population studies of asteroids. However, an outstanding missing element in the understanding of asteroid evolution was a timeline — at least until dynamical methods were developed for estimating family age (*e.g.* Marzari *et al.* 1995; Vokrouhlický *et al.* 2006a,b; Nesvorný *et al.* 2002). The combination of family ages and colors based on remote observations led to the Jedicke *et al.* (2004) relationship between an asteroid surface’s color and its age. We will define the ‘color’ of an asteroid as a linear combination of filter magnitudes. It is correlated with spectral slope (Willman *et al.* 2008). An independent measure of an asteroid’s age depends on its size — the surface of a large asteroid remains intact longer than a small one because it suffers fewer catastrophic disruptions.

The age of an asteroid family can be determined by several dynamical methods, including family size frequency distribution (SFD) modeling, global MB SFD modeling, modeling of family spreading via thermal forces, and backward numerical integration of orbits (Nesvorný *et al.* 2005). A combination of these methods provides age estimates for about 20 S- and C- complex families.

Until recently, few families were known to be younger than ten Myr. Prior to 2006 there were only two such S-complex families, Karin and Iannini, but in that year Nesvorný *et al.* (2006a) and Nesvorný and Vokrouhlický (2006b) identified four small genetic clusters of asteroids aged < 1 Myr. Two years later Pravec *et al.* (2009) and Vokrouhlický and Nesvorný (2008) discovered even younger dynamical pairs of asteroids that separated < 500 kyr ago.

The ensemble of all family asteroid ages as determined by orbital dynamical calculations spans four orders of magnitude and is the first factor required to understand the rate of space weathering using the age-color relationship.

The second factor was color. A conundrum for three decades has been the mismatch between the spectra of the most common meteorites (ordinary chondrites) and their most likely source (inner main belt S-complex asteroids). The space weathering hypothesis was postulated (Chapman and Salisbury 1973) as a means of reconciling the bright, relatively blue spectra with deep absorption bands of ordinary chondrites and the dark, red spectra with shallow absorption bands of S-complex asteroids. It proposes that the surface colors of

asteroids of the same mineralogy will change in a systematic way with airless exposure to the space environment.

The rate of color change on S-complex asteroids has been measured only within the last decade, providing models of surface reddening rate and color range (Willman *et al.* 2010, 2008; Nesvorný *et al.* 2005; Jedicke *et al.* 2004). Space weathering may be due to a combination of mechanisms that could include solar protons or heavier ions, electrons, ultra-violet radiation, micrometeorites, and cosmic rays (see e.g. Chapman (2004) and references therein). However here, as in Willman *et al.* (2010), we are primarily concerned with the phenomenology of space weathering rather than its cause.

Some recent space weathering models have assumed that the amount of unweathered surface will decay exponentially over time (Willman *et al.* 2010; Jedicke *et al.* 2004). One would expect this result if the flow of the weathering agent was constant, an approximation that is probably valid over long periods of time. Willman *et al.* (2010) assume that at the nanometer scale a part of the surface is either unweathered or weathered and that the two states have distinct colors. The physical motivation for this assumption is the metallic iron film deposited on surfaces of nanophase silicate grains under bombardment by pulsed lasers (Sasaki *et al.* 2001) or ion sputtering (Loeffler *et al.* 2009).

Even as an asteroid’s surface ages, weathered surface is transformed back to an unweathered state by regolith gardening at an entirely different rate due to micrometeorites, impact ejecta, seismic shaking, electrostatic levitation, etc. With both weathering and gardening in mind Willman *et al.* (2010) developed their ‘dual τ ’ model to describe the changing colors of S-complex asteroids as a function of age, the time since the family was created in a catastrophic collision that generated a fresh surface on all family members. The name ‘dual τ ’ captures the usage of independent characteristic times for both space weathering τ_w and regolith gardening τ_g . Their model extended the single τ model of Willman *et al.* (2008) and Jedicke *et al.* (2004) by including young clusters in the analysis and by explicitly including the physics of regolith gardening. The dual τ model yielded exponential characteristic times for weathering and gardening of $\tau_w = 960 \pm 160$ Myr and $\tau_g = 2000 \pm 290$ Myr respectively.

The dual τ weathering time is consistent with four other results. Pieters *et al.* (2000) used colors of craters dated by radiometry and cosmic ray exposure ages to determine that space weathering on the moon happens within 100-800 Myr. This corresponds to a space weathering time of 600-4800 Myr in the MB assuming the cause is primarily solar in origin and the effect drops off as $1/r^2$.

Similarly, Veverka *et al.* (1996) found that craters on (243) Ida are bluer than their surrounding background terrain. The craters correspond to freshly exposed and unweathered

regolith while other parts of the asteroid’s surface indicates an age of about 1 Gy (Greenberg *et al.* 1996). The wide range in diameters (a proxy for crater age) of blueish crater suggests that the space weathering time must be long.

In lab experiments Sasaki *et al.* (2001) measured a weathering time of 100 Myr at 1 AU based on laser bombardment of olivine samples (equivalent to 600 Myr in the MB) and this result was confirmed by Brunetto *et al.* (2006).

However, discrepant results include Loeffler *et al.* (2009) who measured a weathering time of only 0.005 Myr at 1 AU based on He ion bombardment of olivine powder. Brunetto *et al.* (2006) summarize ion irradiation experiments finding a reddening time scale of order 1 Myr. Vernazza *et al.* (2009) propose a two-stage process with the first accounting for most of the weathering and occurring in < 1 Myr.

An independent surface age estimate can be determined from an asteroid’s size and its probability of catastrophic disruption *e.g.* Bottke *et al.* (2005). Asteroid surfaces are completely reset during catastrophic disruptions by impactors with diameters that are at least a few per cent of the target’s diameter while smaller impactors will only have local surface effects. Thus, the rate of catastrophic disruption of asteroids depends on their size frequency distribution (SFD) — the larger the asteroid the longer it will survive catastrophic disruption. The SFD can be determined with observations for large objects or through simulating MB collisional evolution that is constrained by the observational results *e.g.* Bottke *et al.* (2005). The interval between catastrophic disruptions as a function of size can only be determined from simulations.

In this work we use a sample of asteroids with known sizes and colors to fit a color-age distribution to the independent size-age distribution using an ‘enhanced dual τ ’ model. There is no a priori reason the two age distributions must match for any combination of parameters. However, we will show that the size-age and color-age methods are consistent and support both our space weathering model and the collisional evolutionary models. Our enhanced dual τ model will correctly predict the color of fresh ordinary chondritic (OC) material.

2. Data sample

Our goal is to compare independent age distributions determined from the sizes and colors of a sample of asteroids. To isolate the effect of space weathering we use only S-complex asteroids thus reducing the inherent mineralogical variation of the sample but still including OC-like objects as shown by *e.g.* Gaffey *et al.* (1993) and Moroz *et al.* (1996). Thus, we

selected a sample of 97 S-complex asteroids from the Small Main-belt Asteroid Spectroscopic Survey (SMASS) Bus and Binzel (2002) that also have u, g, r, i, z filter magnitudes and absolute magnitudes, H , from the Sloan Digital Sky Survey (SDSS) (Ivezić *et al.* 2002). SMASS provided moderate resolution spectra and definitively identified these asteroids as members of the S-complex. While this sample is smaller than the one in our previous work (Willman *et al.* 2010) it has the advantage that each member has rigorous type identification instead of simply relying on family membership.

We used the SDSS u, g, r, i, z filter magnitudes to assign a color to each asteroid from which we determined its color-based age (color-age). Following Nesvorný *et al.* (2005) the principal component color for an SDSS asteroid is

$$PC_1 = 0.396(u - g - 1.43) + 0.553(g - r - 0.44) + 0.567(g - i - 0.55) + 0.465(g - z - 0.58). \quad (1)$$

Willman *et al.* (2008) showed that PC_1 is correlated with spectral slope where increasing PC_1 corresponds to redder asteroids. Almost all the sample members have $0.15 < PC_1 < 0.82$ with two outliers near $PC_1 = 1.70$. We exclude the outliers because of their extreme colors leaving 95 sample members. Leaving the 2 objects in the sample has little impact on the final result.

We independently determined the asteroid’s ages from their diameters as derived from their absolute magnitudes. The diameter, D , for each asteroid was calculated (Bottke *et al.* 2005) from its absolute magnitude, H , and albedo, p_v , where we used an average albedo of 0.215 ± 0.041 from another sample of 93 S-complex asteroids from Bowell (2008):

$$\frac{D}{\text{km}} = \frac{1329}{\sqrt{p_v}} 10^{-H/5} = 2863 \times 10^{-H/5}. \quad (2)$$

3. Color-ages from the dual τ model

Willman *et al.* (2010) characterized the changing color of an S-complex asteroid’s surface as a function of time with their dual τ model

$$PC_1(t) = PC_1(0) + \Delta PC_1 [1 - U(t, \tau_w, \tau_g)] \quad (3)$$

where

$$U(t, \tau_w, \tau_g) = \frac{e^{-(\frac{1}{\tau_g} + \frac{1}{\tau_w})t} + \frac{\tau_w}{\tau_g}}{1 + \frac{\tau_w}{\tau_g}}. \quad (4)$$

The four parameters, $PC_1(0)$, ΔPC_1 , τ_w , and τ_g were fit to the asteroids’ colors, PC_1 , and ages, t , using the least squares method. They found $PC_1(0) = 0.37 \pm 0.01$, the color

of unweathered surface, $\Delta PC_1 = 0.33 \pm 0.06$, the maximum possible color change, and $\tau_w = 960 \pm 160$ Myr and $\tau_g = 2000 \pm 290$, the characteristic weathering and gardening times respectively.

We can invert eq. 3 to determine an S-complex asteroid’s surface age from its color;

$$T_c = \frac{-1}{\left(\frac{1}{\tau_g} + \frac{1}{\tau_w}\right)} \ln \left[1 - \left(\frac{PC_1(t) - PC_1(0)}{\Delta PC_1} \right) \left(1 + \frac{\tau_w}{\tau_g} \right) \right]. \quad (5)$$

The logarithm in eq. 5 disallows negative arguments that result from color values above the upper limit of

$$PC_{1,max} = PC_1(0) + \frac{\Delta PC_1}{1 + \frac{\tau_w}{\tau_g}}, \quad (6)$$

and restricts the invertible color range to $[PC_1(0), PC_{1,max}]$ with a concomitant restriction in the range of predicted surface ages. This is not a mathematical artifact; in the simple analytic model gardening forestalls net weathering at the equilibrium color of $PC_{1,max}$ and asteroids can not be younger than freshly exposed surface. This exposes a fundamental problem with the dual τ model — fitting a function involves finding the central tendency of the data which leaves outlying points beyond the function range. In our sample of 95 objects about $\frac{1}{3}$ of the colors exceed the allowed range of the model.

Thus, we developed an enhanced model described in the next section that is based upon a probability density function (PDF) relating color and age. The model retains the advantage of incorporating the demonstrated color-age relationship while avoiding the inversion singularities.

4. Color-ages from the enhanced dual τ model

The enhanced dual τ model is a PDF given by

$$z(t, PC_1) = \frac{N}{\sqrt{2\pi\sigma_c^2}} \exp \left[-\frac{(PC_1 - PC_1(t))^2}{2\sigma_c^2} \right] \quad (7)$$

where N is a normalization constant such that $\int \int z \, dPC_1 \, dt = 1$, $PC_1(t)$ is the dual τ model of eqs 3 and 4, and PC_1 and t are free parameters. $PC_1 - PC_1(t)$ is the deviation from the predicted color, $PC_1(t)$, for a given age.

To aid in interpreting the PDF the left side of Figure 1 provides an example of the enhanced dual τ model using a linear time scale — each vertical cross-section at a fixed age, t , is gaussian with its mean at $PC_1(t)$ and a standard deviation in color of σ_c .

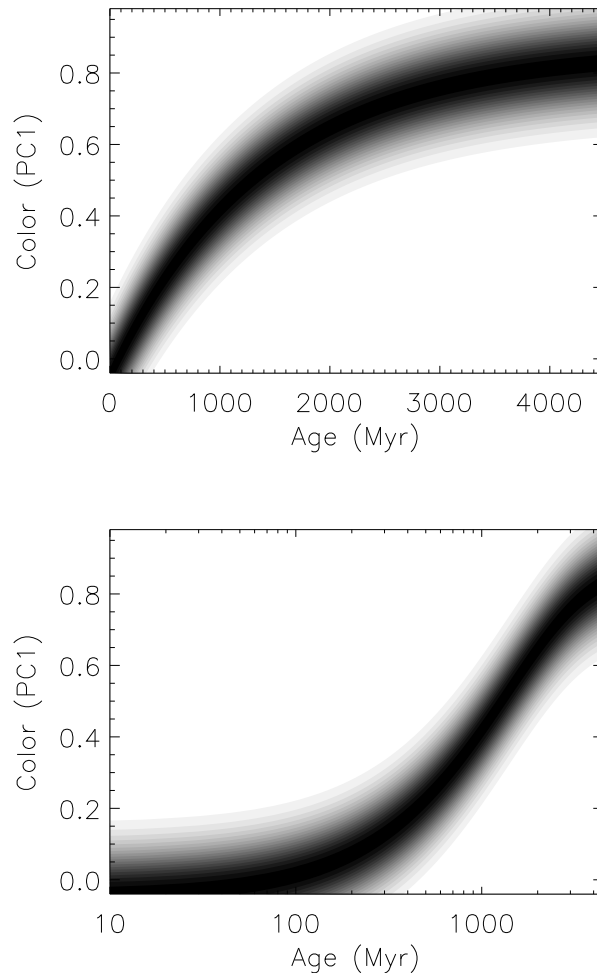


Fig. 1.— Top) The enhanced dual τ model of eq. 7 with $\tau_w = 2050$ Myr, $\tau_g = 4400$ Myr, $PC_1(0) = -0.05$, and $\Delta PC_1 = 1.34$. This set of parameters is explained in §6. Darker regions correspond to higher probability. We use a linear time axis to facilitate the normal interpretation of a pdf with equal areal density signifying equal probability. Bottom) The same function using a logarithmic time scale.

Our choice of σ_c was motivated by the dual τ model that was based on a fit to the average colors of twelve asteroid families. The average rms spread of the families’ colors had a mean of $0.085 \pm 0.017(rms)$ (Willman *et al.* 2010). Given the small deviation between the asteroid families’ rms spread we used a constant $\sigma_c = 0.085$.

Given an S-complex asteroid’s PC_1 the best estimate for its age is the weighted mean

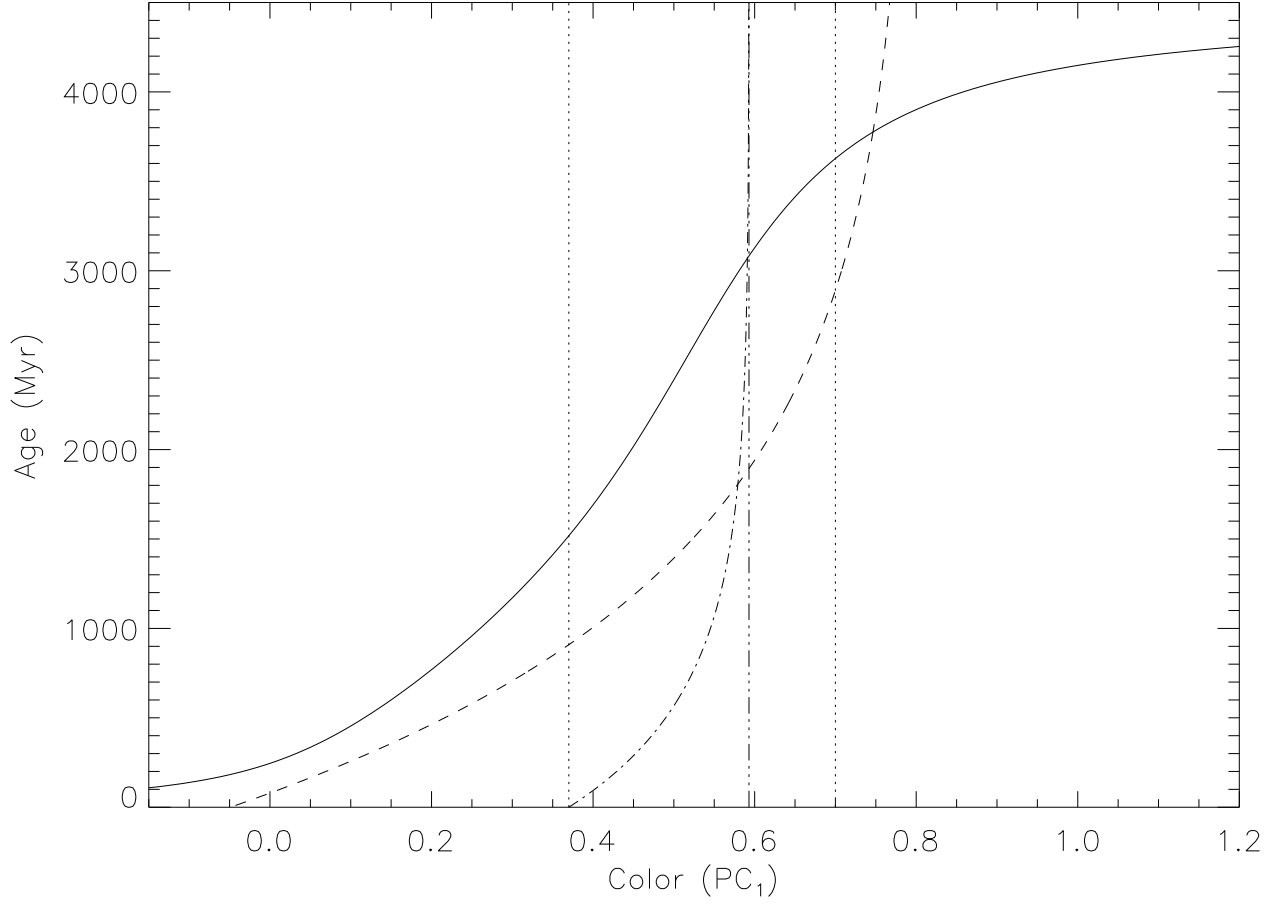


Fig. 2.— (dash dot) The color-age from the inverted dual τ model (eq. 5) which is undefined outside the dotted lines and further constrained at the (dash dot dot) asymptote by gardening. (dashed) The same function using enhanced dual τ model parameters and (solid) the weighted mean color-age from eq. 8 that is defined for all colors. The axes are flipped relative to Figure 1 because age is now considered a function of color instead of vice versa.

color-age

$$\langle T_c(PC_1) \rangle = \frac{\int_0^{t_f} t z(t, PC_1) dt}{\int_0^{t_f} z(t, PC_1) dt} \quad (8)$$

shown in Figure 2. Since $z(t, PC_1)$ is defined for all colors as well as for ages dating back to the beginning of the solar system, t_f , this color-age avoids the inversion singularities of the dual τ model.

However, eq. 8 does not account for the fact that an asteroid i 's color includes a

measurement error, $\Delta PC_{1,i}$, that we model as a gaussian PDF:

$$s_i(PC_1) = \frac{1}{\sqrt{2\pi (\delta PC_{1,i})^2}} e^{-\frac{(PC_1 - PC_{1,i})^2}{2 (\delta PC_{1,i})^2}}. \quad (9)$$

Convolving this PDF with the enhanced dual τ PDF yields the age dependent color-age PDF

$$T_{c,i}(t) = \frac{\int_{-\infty}^{\infty} z(t, PC_1) s_i(PC_1) dPC_1}{\int_0^{t_f} dt \int_{-\infty}^{\infty} z(t, PC_1) s_i(PC_1) dPC_1}. \quad (10)$$

Eq. 10 is not sensitive to t_f . For instance, the difference between using the age of the solar system (4.5 Gyr) and the age of the oldest known asteroid family, Maria, at 3.0 Gyr, results in a negligible shift of the PDF to slightly younger ages.

Summing the color-age PDFs of all the asteroids in our sample yields their combined differential color-age distribution

$$dN_c(t) = \sum_i T_{c,i}(t) dt, \quad (11)$$

the upper envelope of the curves shown in Figure 3. The envelope’s maximum is near 1400 Myr but its mean lies near 2050 Myr due to the tail towards older ages. The envelope’s mean is the analog of the weighted mean given in eq. 8 that corresponds to the enhanced dual τ model parameter τ_w in Table 1.

5. Age distribution from asteroid sizes

In the previous two sections we developed the enhanced dual τ model that enabled us to derive an age distribution from a sample of asteroid colors. We now develop an independent age distribution based on asteroid sizes utilizing the fact that large asteroids are resistant to catastrophic disruptions and therefore have older ages than small asteroids. While large asteroids may be rubble piles reaccumulated in the aftermath of previous collisions (*e.g.* Marzari *et al.* 1995), the age calculated here is the time since the most recent catastrophic collision that last reset the asteroid’s surface age.

A common technique in simulating the MB’s collisional evolution is to numerically model the asteroids’s collisional cascade. The simulations begin with an assumed initial SFD with asteroids distributed across different diameter bins that then evolve as a function of time accounting for the asteroids’ specific energy as a function of diameter. An asteroid that suffers a collision disappears from its bin and its fragments appear in their respective size

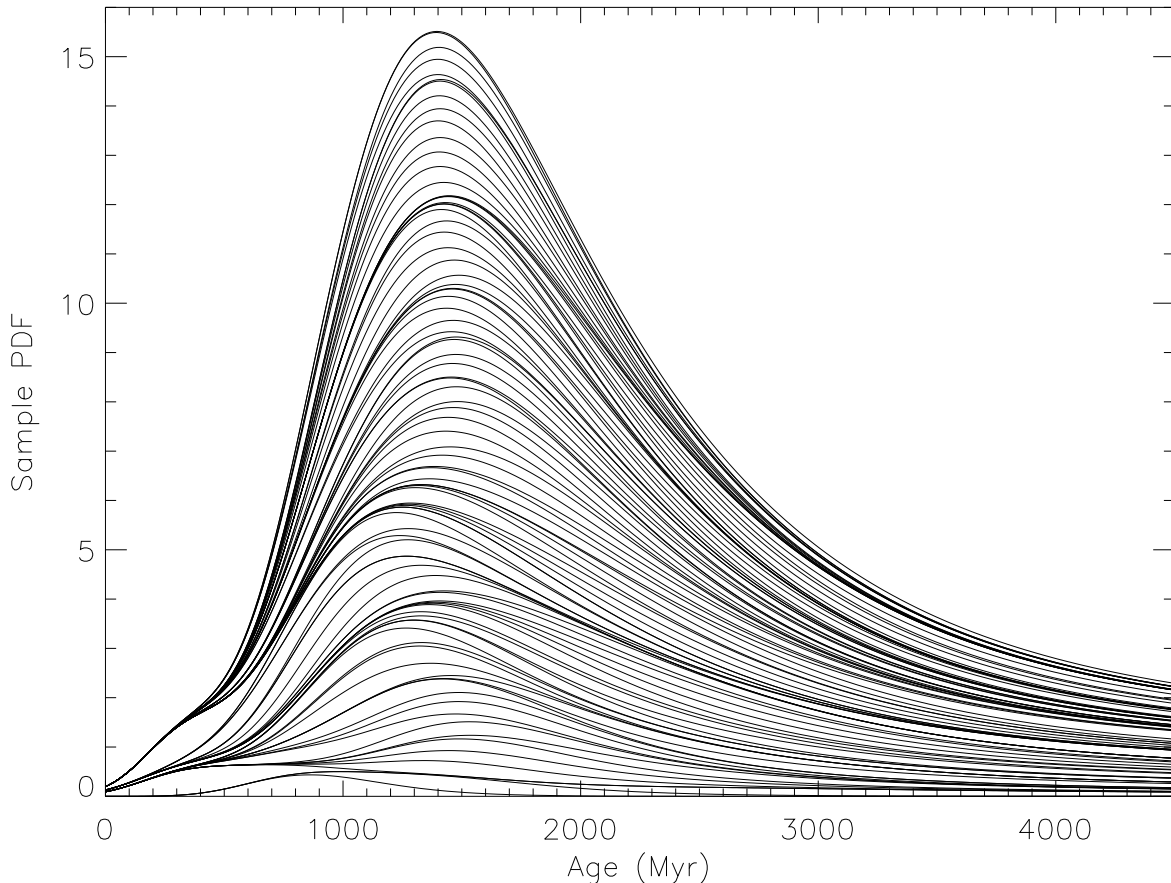


Fig. 3.— Superimposed (stacked) color-age PDFs from eq. 10 for our sample of 95 S-complex asteroids. We used the enhanced dual τ model parameters given in Table 1. The vertical scale is arbitrary.

bins. The simulations are constrained by *e.g.* the current MB SFD, Vesta’s intact surface, the number of large asteroid families, etc, and the fidelity of the models encourages their use in determining the average lifetime of asteroids as a function of diameter.

The average age, \bar{T} , of asteroids in a diameter bin is half the average collisional lifetime in the bin, τ , which in turn is the mean time before destruction by catastrophic collision. The average collisional lifetime is the product of the occupancy, N , and disruption interval, t_{dis} , in the bin:

$$\bar{T} = \frac{\tau}{2} = \frac{N t_{dis}}{2}. \quad (12)$$

We obtained the quantities from the results of a simulation by Bottke *et al.* (2005) as shown

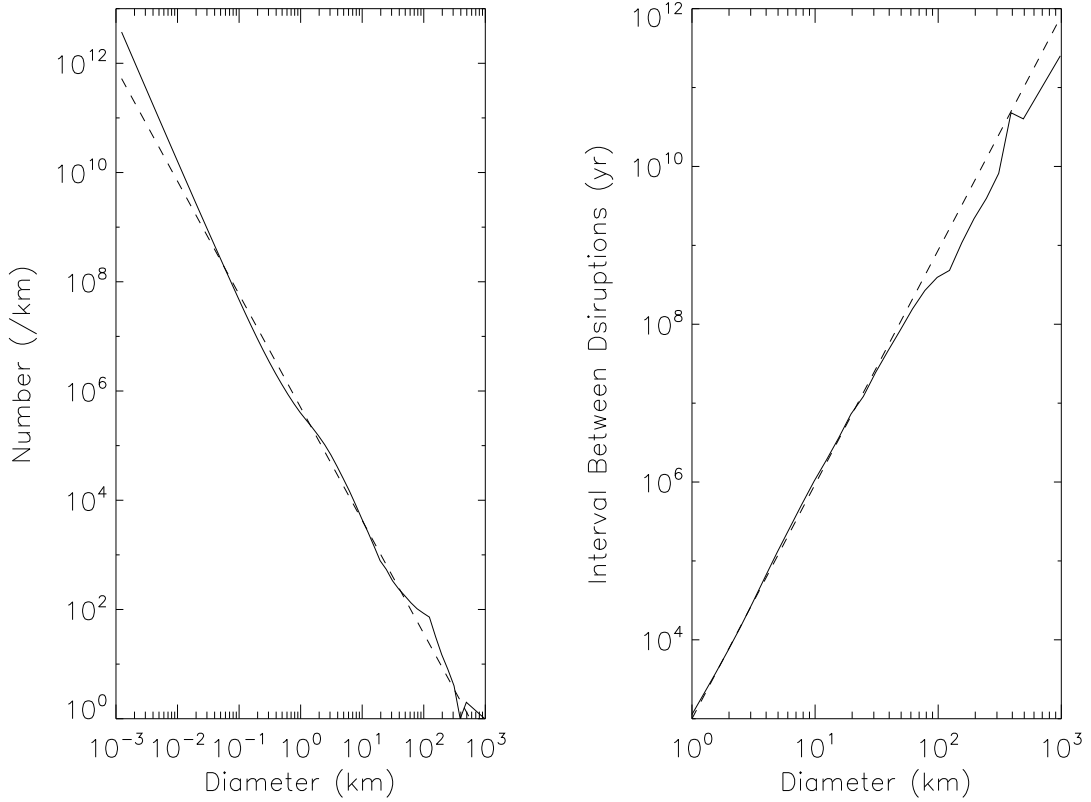


Fig. 4.— From Bottke *et al.* (2005). Left: (solid) The MB differential SFD and (dashed) a power law fit. Right: (solid) The disruption interval as a function of diameter along with (dashed) a power law fit.

in Figure 4.

We used power law fits to N and t_{dis} to calculate the average age as a function of diameter. We restricted the fit to the diameter range of 1-46 kilometers relevant to our 95 asteroids and find that $N \sim 5 \times 10^5 (D/km)^{-2.07} dD/km$ where dD is the diameter bin width, and $t_{dis} \sim 1000 (D/km)^{2.97}$. Combining eq. 2 with the last three equations results in a size-derived age

$$T_s(\text{yr}) = 3.23 \times 10^{(11.0 - 0.18 H)} \quad (13)$$

where we use the observed absolute magnitude as a proxy for diameter.

The size-age distribution for our sample using eq. 13 is shown in Figure 5.

6. Results and discussion

In the previous two sections we described how to obtain an age distribution based on asteroid color (color-age) as well as a diameter dependent age distribution (size-age) derived from collisional evolution models. In this section we fit the color-age PDF to the size-age distribution. The fit yields the enhanced dual τ parameters given in Table 1 and the function shown in Figure 5.

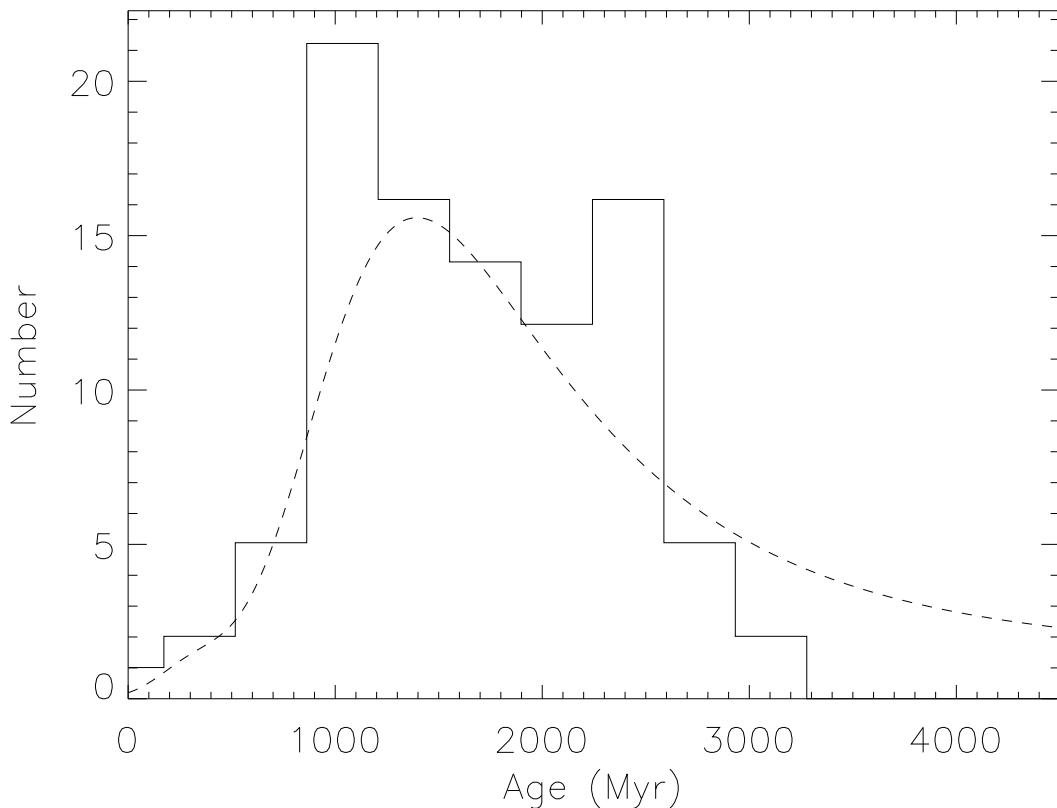


Fig. 5.— (solid) The size-age distribution from eq. 13 for our sample of 95 S-complex asteroids that are in both SDSS and SMASS, (dotted) the fit binned color-age distribution that yields the enhanced dual τ model, and (dashed) the resulting differential color-age distribution from eq. 11.

Our enhanced dual τ model is substantially different in functional form, data sample, and derived parameters from the earlier single and dual τ models. The difference in functional form is particularly relevant to the value and interpretation of the color parameters, $PC_1(0)$ and ΔPC_1 . The broadened range of the color parameters reflect the fact that the PDF of

Model	$PC_1(0)$	ΔPC_1	τ_w	τ_g
Single τ	0.31 ± 0.04	0.31 ± 0.07	570 ± 220	na
Dual τ	0.37 ± 0.01	0.33 ± 0.06	960 ± 160	2000 ± 290
Enhanced dual τ	-0.05 ± 0.01	1.34 ± 0.04	2050 ± 80	4400^{+700}_{-500}

Table 1: The space weathering model parameters for S-complex asteroids derived from average family colors (single τ , Willman *et al.* (2008); dual τ , Willman *et al.* (2010)) or from fitting the color-age PDF to the size-age distribution (enhanced dual τ).

the enhanced dual τ model is not constrained in color and its inversion allows ages to be assigned to asteroids of any color.

We expect $PC_1(0)$, the most probable value for the initial color of unweathered S-complex asteroids, to be bluer than the majority of objects in the complex. It should also match the color of freshly exposed surfaces of ordinary chondrite meteorites in the laboratory. The average color of 329 ordinary chondrite spectra¹ from Cloutis (1994) is $PC_1 = 0.17 \pm 0.39(rms)$ in agreement with our new value of $PC_1(0) = -0.05 \pm 0.01$. The large RMS on the mean meteorite color may be due to differences in the meteorite’s particle sizes and mineralogical subtypes. Thus it is difficult to make a meaningful comparison between the meteorite colors and remotely sensed colors of asteroids with unknown surface regolith structure.

Our long space weathering time of about 2000 Myr is surprisingly different than Vernazza *et al.* (2009)’s result of less than 1 Myr. We are unsure how to reconcile this three order of magnitude difference. Their result relies on several corrections to the colors of asteroid families and it is unclear what age was assigned to freshly cut meteorite surfaces. On the other hand, we fit our model to a sample of less than 100 objects where most span the size range of about 1 – 20 km and an age range of about 100 – 3000 Myr yet we predict, to within 0.5σ , the colors of meteorites that are orders of magnitude removed in both size and age. However we recognize that the meteorites’ RMS color variation is large.

It is also possible that there are two weathering processes having different time scales.

¹Of the 418 ordinary chondrites listed in Cloutis (1994) 329 included spectra, had sufficient wavelength coverage, and were not irradiated. We calculated a spectral slope of $0.10 \pm 0.46/\mu\text{m}$ over the SMASS standard wavelength range of $0.44 - 0.92\mu\text{m}$ and converted it to PC_1 using the transformation derived in Willman *et al.* (2008). Vernazza *et al.* (2009) calculated a slope of $0.01/\mu\text{m}$ over a narrower wavelength range that introduces a systematic offset of $\sim 0.07/\mu\text{m}$ between their slope and this work. Correcting their value with this offset leads to only $0.02/\mu\text{m}$ difference in our slope measurements.

However, our data sample is not large enough to justify exploring whether different weathering time scales are present. The decade of size range we use would not be sensitive to the short timescales because the objects are too large to have experienced recent catastrophic disruption. Clearly, the resolution of the discrepancy between the long and short weathering times requires further work and insight.

In the absence of gardening ΔPC_1 is the maximum possible change of the most probable color of S-complex asteroid surfaces. Gardening constrains the most probable maximum color from eq. 6 to a lower value of $PC_1(0) + \Delta PC_1 / (1 + \frac{\tau_w}{\tau_g}) = 0.91 \pm 0.07$ as illustrated in Figure 2. Figure 1 shows that S-complex asteroids will not reach maximum redness even over the age of the solar system — consistent with our sample having a maximum $PC_1 = 0.82$.

The dual and enhanced dual τ models give weathering times differing by $\sim 6\sigma$ as shown in Table 1. However, they were derived using independent data sets and different fit techniques. The dual τ model was fit to color vs. age data while in this work we fit the inverted enhanced dual τ model to an age distribution determined from sizes. We believe the methodology of the probabilistic enhanced dual τ model is superior because it avoids the color truncation problem of the dual τ model, and attribute the large difference in τ_w between the models to different data sets and small sample size. We expect that in the future larger data samples with good colors along with better collisional evolution models should resolve the discrepancy. The main goal here was to compare the consistency of ages from collisional evolution models and the color inversion method. The agreement of the age distributions in Figure 5 accomplishes our goal.

Willman *et al.* (2010) showed that the gardening time calculated there (Table 1, dual τ) was $\sim 7\times$ longer than the resurfacing time calculated from impact rates and cratering physics. The enhanced dual τ model gardening time is yet another $2\times$ longer! The difference in the values is probably due to the same reasons suggested above to account for the difference in weathering times — small sample size and the use of early collisional evolution models to estimate the size-age of the asteroids.

The fidelity of our results to reality depends on the assumptions used in this work. For instance, we have assumed that σ_c , the color width of the PDF as a function of time, is constant and equal to a specific value determined from the RMS color distribution within families, when it may actually vary with age. With a larger sample size and more accurate colors it may be possible to fit σ_c as a function of time.

Probably the largest systematic uncertainty in this work is the assumption that the collisional evolution model is correct as we have fit the color-age to the size-age distribution. Those models depend on several ill-determined inputs including but not limited to 1) the

current MB SFD 2) estimates of the initial SFD after accretion 3) disruption, cratering, and ejecta physics 4) that material strength as embodied in the specific disruption energy, $Q^*(D)$, is independent of mineralogy 5) and that all objects experience the same density and speed of impactors. For instance, the mean semi-major axis of our sample is $2.63 \pm 0.39(rms) \pm 0.04(err)$ AU compared to $2.806 \pm 0.300(rms) \pm 0.001(err)$ AU for the unbiased MB. The difference is because our sample of 95 asteroids came from SMASS that selected bright (and therefore closer on average) asteroids for spectra acquisition and because S-complex asteroids are primarily in the inner MB. The offset between the values is a significant fraction of the width of the MB — the spatial density of asteroids increases with semi-major axis, impact speeds rise, and material strength decreases. Additionally, S-complex asteroids have higher density than C-complex asteroids which will affect their likelihood of disruption. We hope that future collisional evolution models will incorporate more detail to allow a better comparison between space weathering and gardening time estimates.

We also assumed that the space weathering rate is constant. This working assumption is reasonable even if the actual rate oscillates at high frequency relative to our measured rate but could be problematic if there is a secular trend or the rate oscillates slowly. To explore the possibility that the solar induced weathering rate changes with time Rumpf *et al.* (2009) proposes an expedition to investigate the lunar regolith and plan to test their techniques on Hawaiian lavas.

This work has shown that age distributions from collisional evolution and space weathering models are consistent. Further refinement awaits enhancements in the data sets and mechanisms for both models. While our result based on remote observation of asteroids suggests the weathering time is long it is difficult to reconcile with some lab results. When this remaining discrepancy is resolved we will have solved a four decade long search for the link between ordinary chondrites and S-complex asteroids.

7. Conclusion

We used two independent methods to derive similar age distributions for a sample of 95 S-complex asteroids from SMASS that also have u, g, r, i, z filter magnitudes and absolute magnitudes from SDSS. The first method used absolute magnitudes to calculate diameters that are related to age because large asteroids survive longer than small ones. The second method inverted a probabilistic relationship (the enhanced dual τ model) between an asteroid's color and its age. We developed the enhanced dual τ model to avoid a color truncation problem encountered when inverting the dual τ model of Willman *et al.* (2010). We then fit the color-age distribution from the enhanced dual τ model to the size-age distribution and

showed that there is consistency between the two age determination approaches. This was not inevitable given the entirely independent techniques and suggests we are converging on a self-consistent understanding of both the collisional evolution and space weathering models.

The most probable color for fresh S-complex asteroid surface is $PC_1(0) = -0.05 \pm 0.01$ in agreement with the color of ordinary chondrite meteorites of $PC_1(0) = 0.17 \pm 0.39$. While we are encouraged by the agreement between the two values we realize that it is due to the large color range exhibited by the lab spectra of the meteorites. The wide variation in meteorite colors may be due to differences in particle sizes or subtypes and the absolute difference between our prediction and the color of meteorites may be resolved with a better understanding of asteroid surface regolith.

According to our model the most probable color for S-complex asteroids after infinite time in the absence of gardening is $PC_1(0) + \Delta PC_1 = 1.29 \pm 0.04$. The most probable ultimately attainable color including the effect of gardening is $PC_1 = 0.91 \pm 0.07$. Our model indicates that most asteroids will not achieve this redness over the age of the solar system.

The gardening time of 4400^{+700}_{-500} Myr derived here using the enhanced dual τ model is over twice that found in Willman *et al.* (2010) that itself was about $7\times$ their calculated resurfacing time. It may be possible to reconcile the difference using modifications to cratering phenomena proposed by Willman *et al.* (2010).

Based on our small sample of 95 asteroids for which most span a narrow size and age range of about 1 – 20 km and 100 – 3000 Myr respectively we measured a space weathering time of 2050 ± 80 Myr. This is much longer than some results based on particle bombardment experiments that suggest weathering times of less than 1 Myr. We are unable to reconcile the discrepancy with the particle bombardment experiments but it might indicate that protons or He ions are not the primary cause of space weathering in the main belt. We hope that in the future larger data samples combined with improved collisional evolution and space weathering models will solve the problem.

8. Acknowledgments

This work was supported under NSF grant AST04-07134. We thank Mikael Granvik and Bill Bottke for their helpful suggestions and insights.

REFERENCES

- Abazajian, K. et al, 2009. The seventh data release of the Sloan Digital Sky Survey. SDSS DR7 <http://www.astro.washington.edu/ivezic/sdssmoc/sdssmoc.html>
- Adams, J.B., McCord, T.B., 1971. Alteration of lunar optical properties: age and composition effects. *Science*, 171, 567-571.
- Asphaug, E., Ryan, E.V., Zuber, M.T., 2002. Asteroid interiors. In: Bottke, W.F. Cellino, A., Paolicchi, P. Binzel, R.P., Editors, 2002. *Asteroids III*, Univ. of Arizona Press, Tucson, AZ, pp. 463-484.
- Bowell, E., 2008. Astorb. <ftp://ftp.lowell.edu/pub/elgb/astorb.html>
- Binzel, R.P., Dmitrij, F.L., Martino, M.D., Whiteley, R.J., Hahn, G.J., 2002. Physical properties of near-Earth objects. In: Bottke, W.F., Cellino, A., Paolicchi, P., Binzel, R.P. (Eds.), *Asteroids III*, Univ. of Arizona Press, Tucson, pp. 255-271.
- Binzel, R.P., Rivkin, A.S., Stuart, J.S., Harris, A.W., Bus, S.J., Burbine, T.H., 2004. Observed spectral properties of near-Earth objects: results for population distribution, source regions, and space weathering processes. *Icarus* 170, 259-294.
- Bottke, W.F., Durda, D.D., Nesvorný, D., Jedicke, R., Morbidelli, A., Vokrouhlický, D., Levison, H., 2005. The fossilized size distribution of the main asteroid belt. *Icarus* 175, 1, 111-140.
- Bottke, W., Chapman, C., 2006. Determining the Main Belt Size Distribution Using Asteroid Crater Records and Crater Saturation Models. In: Mackwell, S., Stansbery, E. (Eds.), 37th Annual Lunar and Planetary Science Conference, L.P.I.Tech.Report 37, 1349.
- Brunetto, R., Romano, F., Blanco, A., Fonti, S., Martino, M., Orofino, V., Verrienti, C., 2006. Space weathering of silicates simulated by nanosecond pulse UV excimer laser. *Icarus* 180, 546-554.
- Brunetto, R., Vernazza, P., Marchi, S., Birlan, M., Fulchignoni, M., Orofino, V., Strazzulla, G., 2006. Modelling asteroid surfaces from observations and irradiation experiments: the case of 832 Karin. *Icarus* 184, 327-337.
- Bus, S.J., Binzel, R.P., 2002. Phase II of the Small Main-Belt Asteroid Spectroscopic Survey, The Observations. *Icarus* 158, 106-145.
- Bus, S.J., Binzel, R.P., 2002. Phase II of the Small Main-Belt Asteroid Spectroscopic Survey, A Feature-Based Taxonomy. *Icarus* 158, 146-177.

- Cellino, A., Zappala, V., Doressoundiram, A., Di Martino, M., Bendjoy, Ph., Dotto, E. Migliorini, F., 2001. The Puzzling Case of the Nysa-Polana Family. *Icarus* 152, 225-237.
- Chapman C.R., Salisbury, J.W., 1973. Comparison of meteorite and asteroid spectral reflectivities. *Icarus* 19, 507-522.
- Chapman C.R., Morrison, D., Zellner, B., 1975. Surface properties of asteroids - A synthesis of polarimetry, radiometry, and spectrophotometry. *Icarus* 25, 104-130.
- Chapman, C.R., 2004. Space Weathering of Asteroid Surfaces, *Annu. Rev. Earth Planet. Sci.*, 32, 550-551.
- Chapman, C., Merline, W., Thomas, P., Joseph, J., Cheng, A., Izenberg, N., 2005. Impact History of Eros: Craters and Boulders, *Icarus* 155, 104-118.
- Chapman, C.R., Enke, B., Merline, W.J., Nesvorný, D., Tamblyn, P., Young, E.F., Olkin, C., 2007. Young Asteroid 832 Karin Shows no rotational spectral variations. *Icarus* in press.
- Clark B. F., Hapke B., Pieters C., Britt D., 2002. Asteroid Space Weathering and Regolith Evolution. In: Bottke, W.F., Cellino, A., Paolicchi, P., Binzel, R.P. (Eds.), *Asteroids III*, Univ. of Arizona Press, Tucson, pp. 585-599.
- Cloutis, E.A., 1994. Brown University Keck/NASA Relab Spectra Catalog, <http://lf314-rlds.geo.brown.edu/>.
- Dohnanyi, 1971. Fragmentation and distribution of asteroids. In: *Physical studies of minor planets*, Gehrels, T., Editor, 1971. NASA Special Publication 267, pp. 263-295.
- Durada, D., Greenberg, R., Jedicke, R., 1998. Collisional models and scaling laws: a new interpretation of the shape of the main-belt asteroid size distribution. *Icarus* 135, 431-440.
- Fevig, R., Fink, U., 2007. Spectral observations of 19 weathered and 23 fresh NEAs and their correlations with orbital parameters. *Icarus* 188, 175-188.
- Fowler, J., Chillemi, J., 1992. IRAS asteroid data processing. In: Tedesco, E. (Ed.), *The IRAS Minor Planet Survey*. Phillips Laboratory, Nanscom Air Force Base, MA, 176-189. Tech. Report PL-TR-92-2049.
- Gaffey, M., Burbine, T., Piatek, J., Reed, K., Chaky, D., Bell, J., Brown, R., 1993. Mineralogical variations within the S-type asteroid class. *Icarus* 106, 573-602.

- Gladman, B., Michel, P., Froeschle, C., 2000. The Near-Earth Object Population. *Icarus* 146, 176-189.
- Greenberg, R., Bottke, W., Nolan, M., Geissler, P., Petit, J., Durda, D., Asphaug, E., Head, J., 1996. Collisional and dynamical history of Ida. *Icarus* 120, 1, 106-118.
- Hapke, B., 2000. How to turn OC's into S's: space weathering in the asteroid belt. *Lunar and Planetary Science*, 31, 1087.
- Hardorp, J., 1978. The Sun among the Stars. *A&A* 63, 383-390.
- Hinrichs, J., Lucey, P., 2002. Temperature-Dependent Near-Infrared Spectral Properties of Minerals, Meteorites, and Lunar Soil. *Icarus* 155, 169-180.
- Hirayama, K., 1918. Groups of asteroids probably of common origin. *AJ* 31, 185-188.
- Hiroi, T., Vilas, F., Sunshine, J., 1996. Discovery and Analysis of Minor Absorption Bands in S-Asteroid Visible Reflectance Spectra. *Icarus* 119, 202-208.
- Holsapple, K., Glibin, I., Housen, K., Nakamura, A., Ryan, E., 2002. Asteroid impacts: laboratory experiments and scaling laws in Asteroids III, Bottke, W., Cellino, A., Paolicchi, P. Binzel, R., editors, University of Arizona Press, Lunar and Planetary Institute.
- Ivezić, Ž., Goldston, J., Finlator, K., Knapp, G., Yanny, B., McKay, T., Amrose, S., Krisciunas, K., Willman, B., Anderson, S., and 32 others, 2000. Candidate RR Lyrae stars found in Sloan Digital Sky Survey Commissioning Data. *AJ*, 120, 963-977.
- Ivezić, Ž., Jurić, M., Lupton, R. H., Tabachnik, S., Quinn, T., 2002. Asteroids Observed by The Sloan Digital Survey. In: Survey and Other Telescope Technologies and Discoveries, Tyson, J.A., Wolff, S. (Eds.), Proc. SPIE, 4836, pp. 98-103.
- JPL Small-Body Database, 2009. <http://ssd.jpl.nasa.gov/sbdb.cgi>.
- Jedicke, R., Metcalfe, T., 1998. The orbital and absolute magnitude distributions of main belt asteroids. *Icarus*, 131, 245-260.
- Jedicke, R., Nesvorný, D., Whiteley, R.J., Ivezić, Ž., Jurić, M., 2004. An age-colour relationship for main-belt S-complex asteroids. *Nature*, 429, 275-277.
- Krot, A.N., Keil, K., Goodrich, C.A., Scott, E.R.D., Weisberg, M.K., 2005. Classification of Meteorites. In: Davis, A.M., Holland, H.D., Turekian, K.K., (Eds.), Meteorites, Comets and Planets, Vol. 1, Treatise on Geochemistry, Elsevier, Oxford, pp. 86-116.

- Loeffler, M., Dukes, C., Baragiola, R., 2009. Irradiation of olivine by 4 keV He⁺: Simulation of space weathering by the solar wind. *JGR*, 114, E03003.
- Lugmair, G., Shukolyukov, A., MacIsaac, C., 1995. The Abundance of ⁶⁰Fe in the Early Solar System. In: Busso, M., Raiteri, D., Gallino, R., (Eds.), *Nuclei in the Cosmos III*, AIPCS 327, 591.
- Marchi, S., Brunetto, R., Magrin, S., Lazzarin, M., Gandolfi, D., 2006. Space weathering of near-Earth and main belt silicate-rich asteroids: observations and ion irradiation experiments. *A&A*, 443, 769-775.
- Marchi, S., Paolicchi, P., Lazzarin, M., Magrin, S., 2006. A general spectral slope-exposure relation for S-type main belt and near-earth asteroids. *AJ*, 131, 1138-1141.
- Marzari, F., Davis, D., Vanzani, V., 1995. Collisional evolution of asteroid families. *Icarus*, 113, 168-187.
- http://people.roma2.infn.it/masi/sdss_mass/sdssmass.txt*
- Moroz, L., Fisenko, A., Semjonova, L., Pieters, C., Korotaeva, N., 1996. Optical Effects of Regolith Processes on S-Asteroids as Simulated by Laser Shots on Ordinary Chondrite and Other Mafic Materials. *Icarus*, 122, 366-382.
- Nakamura, K., Sasaki, S., Hamabe, Y., Kurahashi, E., Hiroi, T., 2001. Laboratory simulation of space weathering: A transmission electron microscopic study - microstructures of the laser irradiated samples. *Lunar and Planetary Science Conference XXXII abstract #1547*.
- Nesvorný, D., Bottke, W.F., Dones, L., Levison, H.F., 2002. The recent breakup of an asteroid in the main-belt region. *Nature* 417, 6890, 720-771.
- Nesvorný, D., Bottke, W.F., Levison, H.F., Dones, L. 2003. Recent origin of the solar system dust bands. *ApJ* 591, 486-497. 720-771.
- Nesvorný, D., Jedicke, R., Whiteley, R.J., Ivezić, Ž., 2005. Evidence for asteroid space weathering from the Sloan Digital Sky Survey. *Icarus* 173, 132-152.
- Nesvorný, D., Vokrouhlický, D., Bottke, W.F., 2006. The Breakup of a Main-Belt Asteroid 450 Thousand Years Ago. *Science*, 312, 1490.
- Nesvorný, D., Vokrouhlický, D., 2006. New Candidates for Recent Asteroid Breakups. *AJ*, 132, 1950-1958.

- Nesvorný, D., Enke, B., Bottke, W.F., Durda, D., Asphaug, E., Richardson, D., 2006. Karin cluster formation by asteroid impact. *Icarus*, 183, 296-311.
- Paolicchi, P., Marchi, S., Nesvorný, D., Magrin, S., Lazzarin, M., 2007. Towards a general model of space weathering of S-complex asteroids and ordinary chondrites. *A&A* 464, 1139-1146.
- Pieters, C.M., Staid, M.I., Fischer, E.M., Tompkins, S., He, G., 1994. A Sharper View of Impact Craters from Clementine Data. *Science* 266, 5192, 1844-1848.
- Pieters, C.M., Taylor, L.A., Noble, S.K., Lindsay, P.K., Hapke, B., Morris, R.V., Allen, C.C., McKay, D.S., Wentworth, S., 2000. Space weathering on airless bodies: Resolving a mystery with lunar samples. *Meteorit. Planet. Sci.* 35, 1101-1107.
- Pravec, P., Vokrouhlický, D., 2009. Significance analysis of asteroid pairs. *Icarus* 204, 580-588.
- Rumpf, E., Fagents, S., Crawford, I., Joy, K., 2009. The preservation of ancient solar wind particles buried beneath lunar basalt flows as determined through heat transfer modeling. AGU Fall Meeting Abstracts, C1290+.
- Sasaki, S., Nakamura, K., Hamabe, Y., Kurahashi, E., Hiroi, T., 2001. Production of Iron Nanoparticles by Laser Irradiation in a Simulation of Lunar-like Space Weathering. *Nature*, 410, 555-557.
- Scott, E., 2006. Meteoritical and dynamical constraints on the growth mechanisms and formation times of asteroids and Jupiter, *Icarus* 185, 72-82.
- Scott, E., 2007. Chondrites and the Protoplanetary Disk, *AREPS* 35, 577-620.
- Scott, E., Bogard, D., Bottke, W., Taylor, G., Greenwood, R., Franchi, I., Keil, K., Moskovitz, N., Nesvorný, D., 2009. Impact Histories of Vesta and Vestoids Inferred from Howardites, Eucrites, and Diogenites. In: Lunar and Planetary Institute Science Conference Abstracts, L.P.I.Tech.Report 40, 2295.
- Sheinis, A.I., Bolte, M., Epps, H.W., Kibrick, R.I., Miller, J.S., Radovan, M.V., Bigelow, B.C., Sutin, B.M., 2002. ESI, A New Keck Observatory Echelle Spectrograph and Imager. *PASP*, 114, 851-865.
- Srinivasan, G., Goswami, J., Bhandari, N., , 1999. 26Al in Eucrite Piplia Kalan: Plausible Heat Source and Formation Chronology. *Science*, 284, 1348.
- Stoughten, C., 191 colleagues, 2002. Sloan Digital Sky Survey: early data release. *AJ* 123, 485-548.

- Strazzulla, G., Dotto, E., Binzel, R., Brunetto, R., Barucci, M.A., Blanco, A., Orofino, V., 2005. Spectral alteration of the meteorite Epinal (H5) induced by heavy ion irradiation: A simulation of space weathering effects on near-Earth asteroids, *Icarus* 174, 31-35.
- Tholen, D.J., 1984. Ph.D. Dissertation. Univ. of Arizona, p. 95.
- Vernazza, P., Binzel, R., Birlan, Fulchignoni, M., Rossi, A., 2009. Solar wind as the origin of rapid reddening of asteroid surfaces. *Nature* 458, 993-995.
- Veverka, P., Helfenstein, P., Lee, P., Thomas, P., McEwen, A., Belton, M., Klaasen, K., Johnson, T., Granahan, J., Fanale, F., Geissler, P., Head, J., 1996. Ida and Dactyl: spectral reflectance and color variations. *Icarus* 120, 66-76.
- Vokrouhlický, D., Broz, M., Bottke, W.F., Nesvorný, D., Morbidelli, A., 2006. Yarkovsky/YORP chronology of asteroid families. *Icarus* 182, 118-142.
- Vokrouhlický, D., Broz, M., Morbidelli, A., Bottke, W., Nesvorný, D., Lazzaro, D., Rivkin, A., 2006. Yarkovsky footprints in the Eos family. *Icarus* 182, 92-117.
- Vokrouhlický, D., Nesvorný, D., 2008. Pairs of asteroids probably of a common origin. *AJ*, 136, 380-290.
- Willman, M., Jedicke, R., Nesvorný, D., Moskovitz, N., Ivezić, Ž., Fevig, R., 2008. Redetermination of the space weathering rate using spectra of Iannini asteroid family members. *Icarus* 195, 663-673.
- Willman, M., Jedicke, R., Moskovitz, N., Nesvorný, D., Vokrouhlický, D., Mothé-Diniz, T., 2010. Using the youngest asteroid clusters to constrain the Space Weathering rate on S-complex asteroids. *Icarus* 208, 758-772.